THESIS FOR THE DEGREE OF LICENTIATE IN
APPLIED ACOUSTICS

Modelling the acoustic performance of slab tracks

JANNIK THEYSSEN

Department of Architecture and Civil Engineering

Division of Applied Acoustics

CHALMERS UNIVERSITY OF TECHNOLOGY

Gothenburg, Sweden 2020

Modelling the acoustic performance of slab tracks
JANNIK THEYSSEN

Thesis for the degree of Licentiate
Series name: Lic / Architecture and Civil Engineering / Chalmers University of Technology

Department of Architecture and Civil Engineering
Division of Applied Acoustics
Chalmers University of Technology
SE-412 96 Gothenburg
Sweden
Telephone: +46 (0)31-772 1000

Cover:
Surface plot of the radiated sound power of a discretely supported rail, indicating high power levels by bright colours over frequency (horizontally) and wavenumber (vertically). The harmonic excitation is a point load vertically on the rail head. The axes are increasing from the bottom left. In the upper-left half of the plane, only near fields are created, which are exponentially decaying and thus not radiating outwards. The lower-right half shows radiation in the far field, where the bright lines roughly follow the dispersion curves of the different waves in the rail. The cut-on frequencies of these waves are visible as vertical lines. The repetitive pattern is an effect of the discrete support. The calculations were carried out using the implementations of the Waveguide Finite Element Method and Wavenumber Boundary Element Method used in this work.

Chalmers Reproservice
Gothenburg, Sweden 2020

Modelling the acoustic performance of slab tracks
Thesis for the degree of Licentiate in Applied Acoustics
JANNIK THEYSSEN
Department of Architecture and Civil Engineering
Division of Applied Acoustics
Chalmers University of Technology

Abstract

Transport is a major contributor to anthropogenic greenhouse gas emissions. Railway transport has a small footprint compared to other means of transport. This is one reason for the construction of new high-speed railway lines world-wide. These lines are often constructed using slab track technology, in which the traditional track configuration of concrete sleepers and ballast is replaced by concrete slabs. In earlier work, it has been found that traffic on slab tracks has higher noise emissions than on ballasted tracks. Rolling noise, radiated from wheels and track, is an important contributor to these noise emissions. To predict the acoustic performance of slab tracks, first, a model for the high-frequency vibration in these tracks is necessary, for which there is currently no standard solution. Further, the effect of the reflective slab track surface on the wheel radiation has not been researched.

In this work, a model for the high-frequency vibrations and acoustic radiation of slab tracks has been developed and implemented. The validity of the dynamic model has been tested on a full-scale test rig. The developed model was then used for researching the influence of track parameters on noise emission. In this investigation, the rail pad stiffness was identified to have a major influence. Besides, a model for the sound radiation of railway wheels over hard reflective surfaces was developed, implemented, and validated. The effect of the slab track surface on the radiation efficiency of the vibrating wheel was evaluated and found negligible. The developed models are steps towards predicting the rolling noise generated by rail vehicles on slab tracks, which is significant both for the planning of new lines and the investigation of potential abatement measures.

Keywords: slab track, railway noise, rolling noise, numerical modelling, acoustic optimisation

Preface

Anything that grows in nature can only reach its full potential when the surrounding conditions for its growth are ideal. Likewise, the work and development towards a Ph.D. will be most fruitful in a supportive environment. I would like to acknowledge the ones who are creating and sharing such an environment with me.

Thank you, Wolfgang and Astrid, you are an essential part of this environment. Wolfgang, I am grateful for our countless discussions in which your experience and knowledge helped to keep things in perspective, which made me grow both in my research and personal life. Thank you, Astrid, for your competent support, your comprehensive feedback, and your belief in my work, which makes it a pleasure to work with you.

Dear colleagues at Applied Acoustics, thank you for all the small chats and deep thoughts during coffee or tea, in between doors, in hallways, or (sometimes) on blackboards. Carl, thanks not only for all the idea-bouncing and maths-talk. Thank you Börje, Jens, Jens, Patrik, Hannes, Carmen, Fati, and Georgios, for your important contributions to our environment.

The work in this thesis has been accomplished from September 2019 to May 2020 at the Division of Applied Acoustics at Chalmers University of Technology within the research project VB13 "Noise from slab tracks". It has been a part of the research activities within the Centre of Excellence CHARMEC (CHAlmers Railway MEChanics). In particular, the support from Trafikverket (the Swedish Transport Administration) is acknowledged. Dear colleagues at CHARMEC, thank you for your support. Thank you, Emil, your systematic approach to problem solving, skilled diplomacy, and patience were vital. Jens, I am thankful for your encouragement, critical feedback, and expertise. I very much appreciate the fruitful discussions and valuable inputs from you, Anders Ekberg, Andreas Andersson, and Martin Li. Thank you, Monica Waaranperä and Martin Schilke, for seamless communication. I look forward to continued cooperation with all of you.

Dear friends and Ph.D.-colleagues at Chalmers, thank you for being such an active part of my environment, making me thrive in so many ways. To my friends in Germany and Sweden, I am grateful to have you in my life. And, most importantly, thanks and love to my family, unconditionally on my side in the ups and downs which life offers me to grow.

Steninge, May 2020

Jannik Theyssen

Thesis

This thesis consists of an extended summary and the following appended papers:

Paper A J. Theyssen, A. Pieringer and W. Kropp. The Influence of Track Parameters on the Sound Radiation from Slab Tracks. *Proceedings of the 13th International Workshop on Railway Noise (IWRN 2019)*, Ghent, Belgium (2019).

Paper B F. Fabre, J. Theyssen, A. Pieringer and W. Kropp. Sound Radiation from Railway Wheels including Ground Reflections: A half-space formulation for the Fourier Boundary Element Method. *Submitted for international publication* (2020).

Paper C J. Theyssen, E. Aggestam, S. Zhu, J. Nielsen, A. Pieringer and W. Kropp. Calibration and validation of two dynamic slab track modelling approaches using measurements from a full-scale test rig. *To be submitted for international publication* (2020).

The appended papers were prepared in collaboration with the co-authors. The author of this thesis was responsible for the major progress of the work including taking part in the planning of the papers, developing the theories and the numerical implementation, performing the numerical simulations and writing the papers. The development of parts of the methodology and parts of the implementation leading up to **Paper B** were carried out by François Fabre. The planning and realisation of the measurements, the numerical simulations and the writing of **Paper C** were conducted in close collaboration with Emil Aggestam.

Contents

Abstract i

Preface iii

Thesis v

Contents vii

I Extended summary 1

1 Introduction 1
1.1 High-speed railway lines and slab tracks . . . 1
1.2 Challenges: Noise from traffic on slab tracks . . . 3
1.3 Overview . . . 4
1.3.1 Context . . . 4
1.3.2 Objectives . . . 6
1.3.3 Outline . . . 6

2 The rolling noise generated on slab tracks compared to ballasted tracks 7

3 Slab track dynamics and noise modelling 8
3.1 Slab track systems . . . 8
3.2 Slab track dynamics . . . 10
3.2.1 WFE rail on simple support . . . 12
3.2.2 WFE rail on WFE slab . . . 17
3.3 Noise from slab tracks . . . 19

4 Railway wheel dynamics and noise modelling 20
4.1 Railway wheel dynamics . . . 20
4.2 Noise from railway wheels . . . 21

5 Summary of appended papers 24

6 Conclusions 26

7 Future Work 27

References 28

II Appended Papers A–C 33

Part I
Extended summary

1 Introduction

1.1 High-speed railway lines and slab tracks

In 2017, 24.6% of the total greenhouse gas (GHG) emissions in the European Union (EU) originated from transportation [1]. This sector is therefore a key focus to reducing GHG emissions. According to a 2011 White Paper by the European Commission [2], carbon emissions due to transport are to be reduced by 60% by 2050 with respect to 1990.

Figure 1.1 presents the total travelled distance in the EU by mode of transportation. While railway transport shows a constant, moderate increase, there is a large increase in air transport in the past decade. Considering the large CO_2 emissions from air transport per passenger-km in comparison to other means of transport, this indicates a need for a more resource efficient transport system[1]. High-speed rail connections could provide a viable alternative to some domestic flights for most European countries.

Today, rail transport is the fourth largest mode of passenger transport in the EU and plays a significant role in many other countries. In 2017, railways covered a share of 7.8% of passenger transport in the EU, of which 27% were high-speed connections [1]. It is clear that a more railway-focused transport system is envisioned by the EU: In the 2011 White Paper by the European Commission a key goal is a 50% shift of medium distance intercity passenger and freight journeys from road transport to rail and water-borne transport [2]. One step to achieving this shift is the continued construction and development of high-speed railway lines.

The development of high-speed railway lines started with the Japanese Shinkansen railway line, operating at a speed of 210 km/h, connecting Tokio and Osaka [3]. The definition of "high speed" has since then been increased to 250 km/h, and high-speed railway lines were introduced in many other countries such as France, Germany, and China [3]. In the last decade, the global traffic in high-speed railway lines has grown substantially, from 245 billion passenger-km (pkm) in 2010 to 956 billion pkm in 2018. This growth is to the largest part a product of the increased Chinese railway network (46 billion pkm in 2010 to 680 billion pkm in 2018) [4].

Ballasted tracks were used in the original Shinkansen line, building on earlier experience with this common type of track. Ballasted tracks are designed such that the rails are mounted on sleepers, which rest on a ballast layer. Sleepers are concrete or wooden

[1] The UIC states the equivalent carbon dioxide emissions for a 600 km trip to be 93 kg for air transport, 67.4 kg for transport by private car and and 8.1 kg for railway transport [3].

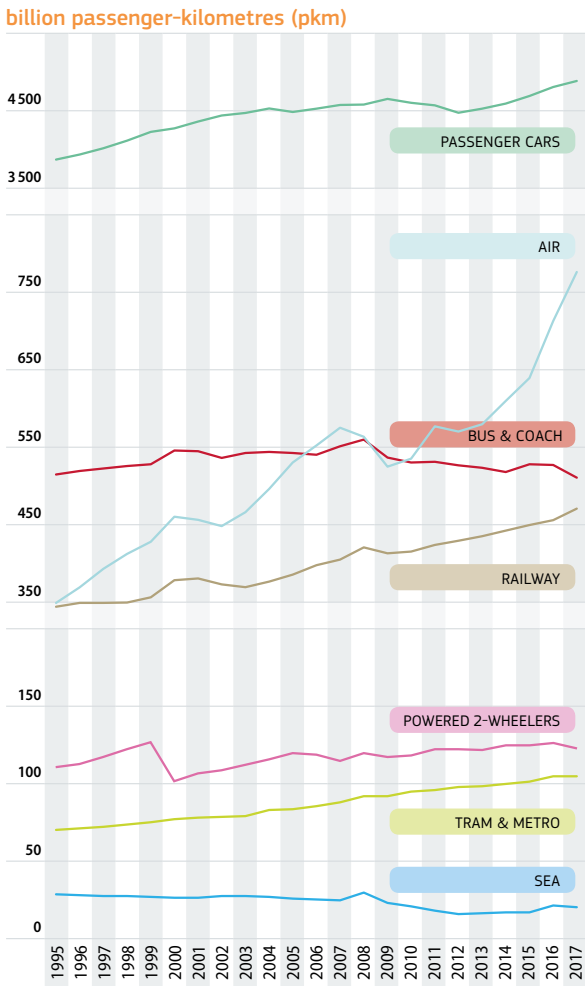

Figure 1.1: EU-28 performance for passenger transport 1995-2017, from [1].

beams which are placed perpendicularly to the track direction such that they connect both rails. The ballast layer can undergo geometrical alteration during use, creating a need for frequent and costly maintenance [5, 6].

In order to mitigate this geometrical deterioration, new tracks were developed in which the sleepers were replaced with large concrete panels. These so-called slab tracks or ballastless tracks are railway tracks in which the rails are supported by a solid, often concrete structure that connects both rails and extends parallel to the track. The stiffer support leads to a longer lifetime and reduced maintenance, and therefore higher availability of the line [6]. Slab track sections were first introduced into the Shinkansen line in 1972 and are now extensively used for high-speed railway lines in e.g. China, Japan and Germany.

There are challenges in the design of new high-speed railway lines using slab tracks. A main factor next to the higher construction costs are the lower noise and vibration absorption of this type of track compared to ballasted track [6]. This can lead to a higher noise exposure for residents.

1.2 Challenges: Noise from traffic on slab tracks

Traffic noise is a major health concern. Its effect on humans is quantified by indicators like the L_{den}, a noise indicator used to assess annoyance during day, evening and night, and the L_{night}, which is used to assess sleep disturbance. These parameters measure a long-term average exposure on residents as defined in ISO 1996-1:2016(E) [7]. The World Health Organisation (WHO) recommends an exposure of less or equal to ($L_{\text{den}}/L_{\text{night}}$) 53/45 dB for road traffic, 54/44 dB for rail, 45/40 dB for air traffic. However, according to the UIC, more than 18 million people are exposed to noise levels (L_{den}) larger than 55 dB [8]. The L_{den} indicator increases with an increasing number of trains per day on a given track. In combination with the envisioned railway-focussed transport, a reduction of $L_{\text{den}}/L_{\text{night}}$ can only occur by reducing or absorbing the noise radiated by individual vehicles and tracks.

To reduce the noise radiated by individual vehicles, an understanding of the processes involved in noise generation is necessary first. In general, railway rolling noise occurs due to the interaction of the rail and the moving wheel, in which the surface roughness of both components excites structural vibrations and ultimately noise. The vertical excitation of wheel and rail is the predominant source for rolling noise [9]. The two components interact in the contact patch, a small area in which the roughness of the surfaces influences the vibrations [10]. Wavelengths that are short in comparison to the contact patch, or in the same order as the contact patch, excite the wheel/rail system less effectively than longer wavelengths [11, 10]. This is called the contact filter effect. If the interaction in the contact patch is simplified to a single Hertzian spring in numerical models, the contact filter effect has to be added explicitly [12, 13, 14, 10]. The wavelength in the roughness spectrum is coupled to the excited frequency by the speed of the moving wheel. For high-speed railway lines, it is known that the noise from the rails and the wheels dominates over other sources, for example aerodynamic noise from the pantograph, at

least up to 300 km/h [15, 16], at relevant frequencies for human perception. Although this is not specific to ballast-less tracks, it shows the necessity to focus on the wheels, the rail and the track as noise sources in a wide speed range.

Some challenges in the understanding and modelling of the radiation from wheels and rails on slab tracks are stated below. The first question when focussing on slab tracks is the comparison to ballasted tracks. Even though extensive measurement campaigns and detailed simulation models have been used to quantify the increase in noise radiation, there is no simple way to quantify the difference between ballasted tracks and slab tracks. Related to this point is a second challenge: a large body of research exists for the key parameters that influence the sound radiation from ballasted tracks. However, it is not clear that these parameters will have the same effect on slab tracks. In order to e.g. evaluate mitigation measures, an investigation of these parameters is relevant. Thirdly, when researching the high-frequency vibro-acoustic properties of slab tracks, accurate numerical models can give further insights. The large size of the structure makes it costly to use detailed numerical models. Finally, with the slab track surface in close proximity to the vibrating wheel, the radiation efficiency of the wheel can be affected. This effect is not as relevant in ballasted tracks, since the ballast does not have an acoustically hard surface (the air in the ballast has absorptive character). This could, for wheels on slab tracks, lead to an increase of the pass-by sound pressure level not only due to the lacking decrease due to ballast absorption but also due to a more efficient sound radiation. These challenges are addressed in the following.

1.3 Overview

1.3.1 Context

This thesis aims to improve modelling approaches to solving vibro-acoustic issues related to rolling noise generation on different slab track. The components involved in the noise generation are the rail, the rail support (i.e. sleepers or a slab) and the wheels. Often, four stages of the calculation process can be found in models. Figure 1.2 shows these four stages in the calculation process.

1. *The frequency response functions* - The dynamic properties of the wheel and the rail are pre-calculated and used in the following two steps. Typical input parameters are the geometry, material data and information about the contact positions. The dynamic response can include support systems, e.g. the wheel suspension or sleepers.

2. *The contact problem* - The complex interaction of the rail and the wheel in their contact needs to take the combination of their individual roughnesses into account. The contact forces can be calculated based on an interaction model, which serve as input to the structural vibrations. Input parameters typically also include the wheel load and vehicle speed.

3. *The structural vibration* - The structural response of the wheel and the rail to the contact forces is calculated using the receptances and forces from the two earlier steps.

4. *The sound radiation* - Based on the vibrations, the sound radiation from both the wheels and the track is calculated. Their contributions are summarised at an observer position.

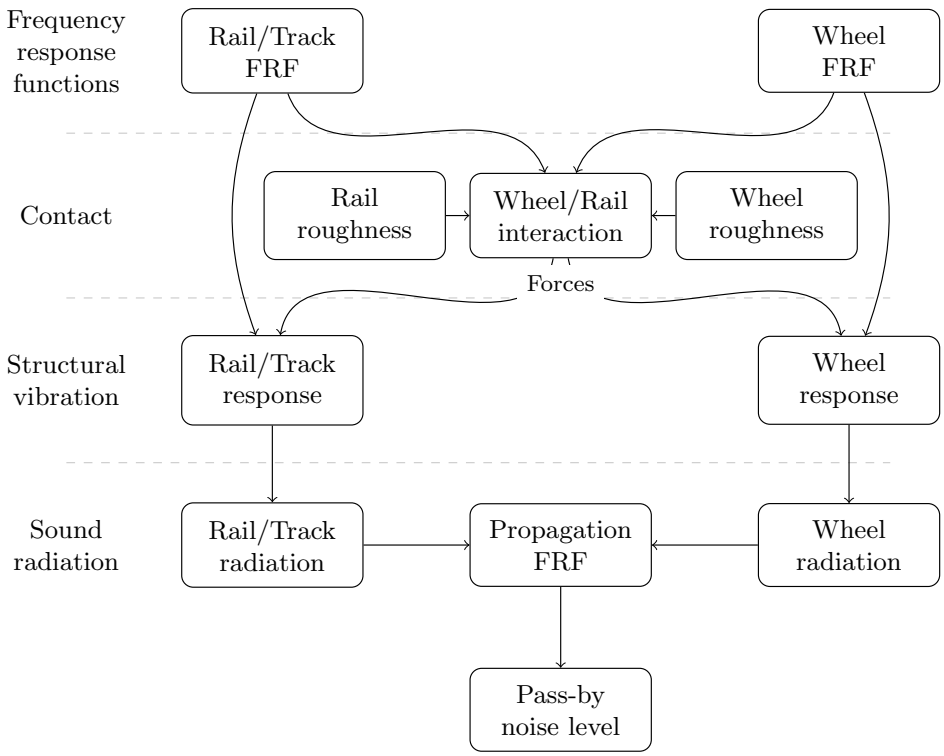

Figure 1.2: Visualisation of the components involved in railway rolling noise modelling. A large focus in this thesis is the evaluation of the frequency response functions (FRF).

A model of this type is visualised by Remington in [17], however the concept is already used in [12]. Every stage in this model can be evaluated using different methods, as e.g. the contact can be solved in frequency or time-domain, and the frequency response functions can be solved using analytical models or numerical models as Finite Element Method (FEM) in spatial or Waveguide FEM (WFEM) in wavenumber-domain. In [17], analytical models are used in all four steps based on earlier research, e.g. by Munjal et al. for the track [18] and for the wheel [19]. A model of this type is also presented in [13], in which numerical models for all stages are introduced. The modularity of this approach

allows e.g. introducing a new type of track or a different wheel radiation characteristic. This modularity is used in this thesis to address the challenges mentioned in Section 1.2.

1.3.2 Objectives

This thesis is focused on the development of appropriate models for the noise radiation from slab tracks and wheels above slab tracks. These models are then applied to deepen the understanding of their acoustic properties. The key objectives are

- to develop a numerical method for predicting the vibration in slab tracks,
- to predict the sound radiation from slab tracks,
- to predict the sound radiation from wheels over reflective surfaces, and
- to identify key track parameters for the noise radiation from slab track.

1.3.3 Outline

This thesis is structured as follows:

Chapter 2 presents existing work about the increase in rolling noise from trains on slab tracks compared to ballasted tracks.

Chapter 3 presents models for the dynamic response of the track. In Section 3.1, an overview over existing slab track systems is presented. Out of these, the most relevant system for this thesis is selected. A methodology for evaluating the dynamic response of this track system is developed in **Paper A** and summarised in Section 3.2. The model is calibrated and validated in **Paper C**. Using this model, a method for calculating the noise emissions from slab tracks is introduced in Section 3.3, which is presented in **Paper A**.

Analogously, in Chapter 4, the wheel dynamics and noise are described. It is focussing on the dynamic response in Section 4.1 and the noise radiation in Section 4.2. This chapter builds on **Paper B**, in which a methodology to simulate the dynamic response as well as the acoustic radiation from railway wheels is developed.

Finally, the appended papers are summarised in Chapter 5. Chapter 6 concludes this work and Chapter 7 gives a perspective on future work.

2 The rolling noise generated on slab tracks compared to ballasted tracks

The research of acoustical differences between ballasted and slab tracks has been a major focus in the last two decades due to the increased application of slab tracks in high-speed railway lines. In the year 2000, the project "acoustical innovative ballast-less track design" (AIFF) carried out in Germany was presented by Diehl et al. [20]. In the publication, it is stated that based on simulations, a significant difference in the noise level between the two track types for interior noise and the structure-borne noise on the rail is found. Further, increased sound radiation from the rails was found in the frequency range 500 Hz to 1500 Hz predominantly due to the higher vibration levels in the rail at these frequencies. The higher vibration level was discovered to be due to the significantly lower damping of the rail due to the lower rail pad stiffness. As a result of this project, an optimised track including a sleeper base with increased damping was presented.

Parallel to that, in the Netherlands, there was the project "Stiller Treinverkeer" (silent railway traffic), focussing on the same issue. It is stated that a ballast-less track is expected to lead to a 3 dB(A) higher noise radiation. With the help of numerical models, an acoustically optimised track was developed [21], which showed a potential reduction of between 4 dB(A) and 6 dB(A) compared to ballasted track. The German prediction model "Schall 03 2006", presented by Moehler et al. [22], estimates an increase of about 4 dB(A) to 2 dB(A) for slab tracks compared to ballasted tracks for an ICE 1, decreasing with increasing speed. In [23], the difference is found to be about 3 dB(A) in sound pressure level when measured at 25 m distance from the track. For one specific case, three factors were identified as reasons for this, being (i) a difference in rail roughness due to different maintenance, (ii) a difference in the track decay rate, and (iii) the change in propagation path due to reflections from the slab. In addition to the lower fastening stiffness, Gautier [6] gives a second reason for the increase in noise radiation from slab tracks. The noise absorption, which the ballast in a ballasted track provides, is replaced with a surface that acts as a pure noise reflector. A recommendation is given to address the noise issue by following a comprehensive system approach in future designs. In [24], these differences are researched based on numerical models. It is found that the resulting differences strongly depend on the initial assumptions about the track, such as the rail roughness and the track decay rate. Furthermore it is pointed out that the ground conditions adjacent to the track affect the pressure spectra.

3 Slab track dynamics and noise modelling

This section covers the track related components of the modelling approach described in Section 1.3.1. First, existing non-ballasted tracks are categorised in Section 3.1. Then, relevant models for the structural vibration and the sound radiation from non-ballasted tracks are discussed in Section 3.2, which includes the model developed in this work. Finally, the developed method of calculating the noise from slab tracks is presented in Section 3.3.

3.1 Slab track systems

In the following, a short overview and categorisation of existing slab track systems is given. For a more extensive description of the tracks, see e.g. Esveld [5]. This summary follows Figure 3.1.

The systems are first categorised by how the rail is supported along the track, which can be either continuous or discrete. Some systems use a continuous rail support. The rail is then either discretely clamped on or embedded in an elastomeric material. Thus, there is no periodic variation in track stiffness as in a discretely supported rail. This lowers the dynamic loads [25]. In embedded rail systems (ERS) as e.g. produced by edilon)(setra or the Balfour Beatty system, the rail is enclosed by an elastic compound, see Figure 3.2a. As shown in [15], this has significant benefits in terms of noise reduction. An example of a system with a discretely clamped and continuously supported rail is the Cocon track [5]. Due to the rail support being poured in-situ, there is little possibility for readjusting the rail, which is one major downside of this system.

In high-speed railway lines built using slab tracks, discrete support systems dominate, either with or without sleepers. These can be differentiated by how the sleepers are mounted. Three types of sleeper mounts are presented in the following. Firstly, one of the more commonly used systems is the RHEDA system, in which the rail is attached by pre-cast twin-block sleepers. The sleepers are embedded in a reinforced concrete slab resting on a hydraulically bonded layer [26]. Secondly, there are designs in which the sleeper is not embedded, for example the Getrac system [27]. Here, pre-stressed concrete sleepers are anchored on an asphalt layer, which rests on several support layers, possibly including hydraulically bonded layers. The sleepers can also be anchored on a concrete panel (Beton-Tragschicht mit Direktauflagerung, BTD). A strength of this system is its fast installation. And thirdly, another approach is to mount individual or twin-block sleepers on an elastic material, which itself is embedded in a concrete panel. This is the case in the STEDEF or Sonneville-LVT systems [6].

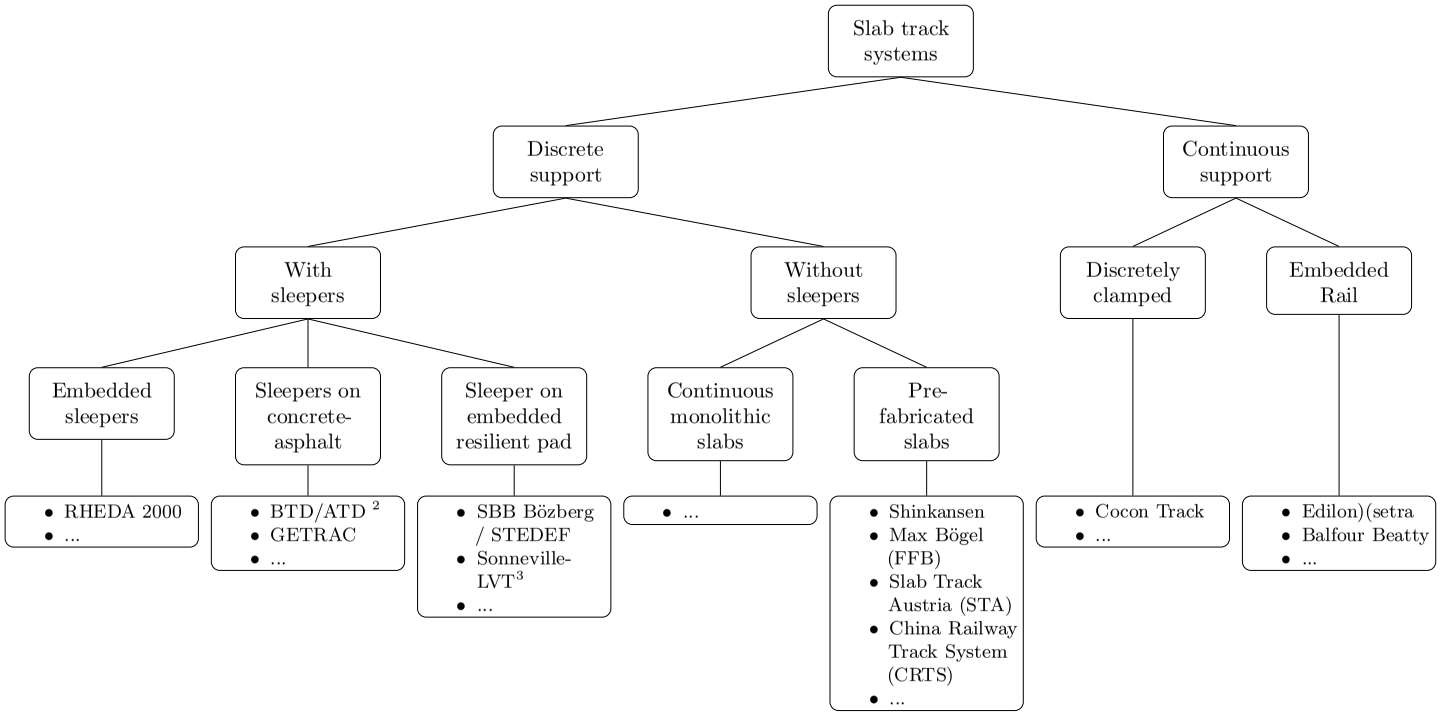

Figure 3.1: Categorisation of slab track systems.

[2]**B**eton-/**A**sphalt **T**ragschicht mit **D**irektauflagerung (Sleepers resting on concrete layer)
[3]Low vibration track

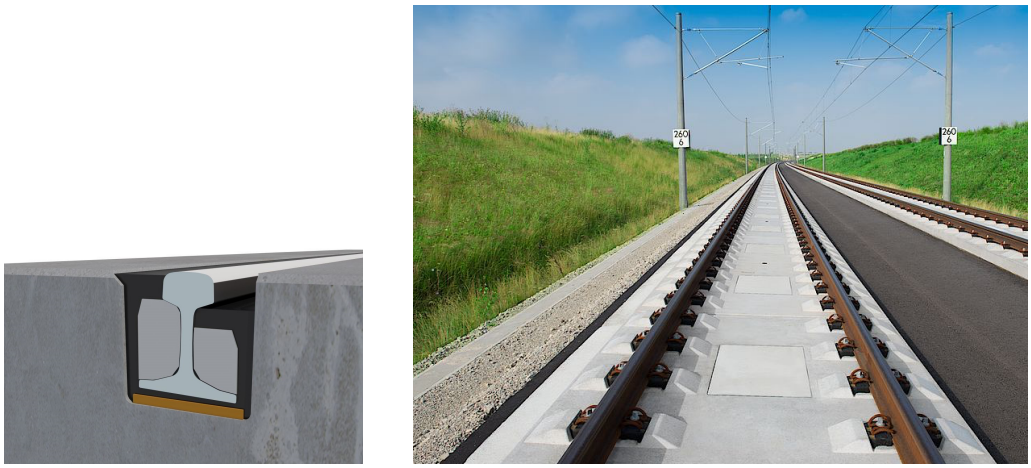

(a) (b)

Figure 3.2: Different types of slab track. (a) A sketch of a continuously supported, embedded rail (from [29]). (b) A slab track system with discrete rail supports without sleepers and pre-fabricated slabs called Slab Track Austria (from [30])

Systems without sleepers can either be continuous monolithic slabs, which are typically produced in-situ, or pre-fabricated slabs. Monolithic structures are rarely used to cover large distances but are well suited for civil structures like bridges [25]. Systems using pre-fabricated slabs are very commonly used in high-speed railway lines [6]. With the introduction of the SHINKANSEN train in Japan in 1964 [3], these systems have been continuously developed. Today, the German Max Bögel system, the Austrian system developed by ÖBB and the company PORR called Slab Track Austria (STA) and the Chinese CRTS series CRTS I – CRTS III are commonly used in high-speed slab track lines worldwide [6, 28]. Figure 3.2b shows an example of the STA system, representing the group of pre-fabricated slabs. In this work, the focus is mainly on the latter types of slab track. Figure 3.3 shows the setup of the CRTS III system, consisting of the pre-fabricated slabs resting on several different base layers. In this system, the slab sections are typically in the order of 5 m in length.

3.2 Slab track dynamics

Different applications require different levels of detail when modelling railway tracks. For the goal of simulating vehicle system dynamics, a (rigid) multi-body dynamics model can be sufficient [6]. This is largely due to the comparatively low upper frequency limit. For in-depth analysis of the structural behaviour of the track, such as internal stresses, a full Finite Element model of the track often necessary [25]. The rail can be approximated by Timoshenko beam elements if the upper frequency limit is not higher than about 1 kHz,

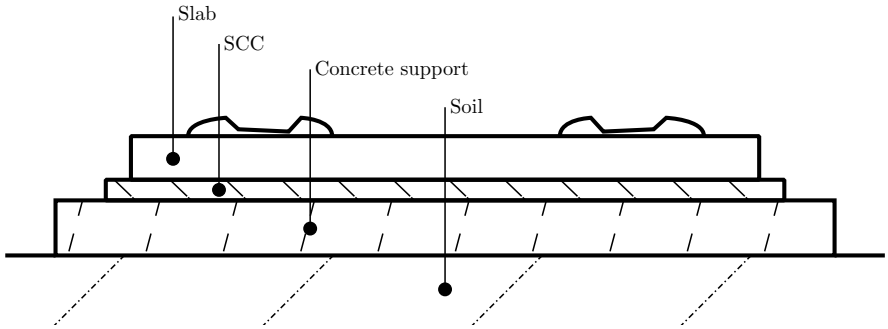

Figure 3.3: Cross section of a CRTS III slab track system. The slab rests on a layer of self-compacting concrete (SCC). Setup according to [28].

since below that, the cross-sectional deformation and vertical/lateral cross-coupling are small [31]. For the application of predicting structural vibrations and simulate noise radiation, the frequency range of human hearing becomes relevant, and therefore the beam model is no longer a good approximation. According to Thompson [15], the largest contributions from the rail to the radiated sound pressure level in a pass-by measurement can be expected below 3 kHz. In this section, numerical models of the structural dynamics of rails, aiming for simulating sound radiation, are presented. Dynamical models for calculating slab track behaviour are not readily available, and an approach to solving this issue is presented in the attached papers.

One of the first numerical models for the structural dynamics of the rail was a finite element (FE) based model that has been introduced by Thompson [32]. Here, a rail section was modelled with shell elements and symmetric and/or anti-symmetric boundary conditions on both ends to represent an infinite extent of the rail. A different FE-based approach, assuming wave propagation along the free rail, was introduced by Gavric et al. [33]. This approach makes use of the fact that the rail has a constant cross-section over its length and it thus acts as a waveguide. This approach is called the waveguide finite element (WFE) method[4]. This has the disadvantage that the rail either needs to be modelled free in space or with a continuous support condition over the whole length. However, in practice, the rail seats provide a coupling of the rail in discrete points along the rail. The issue of the discrete coupling is addressed in the spatial domain for a rail based on Timoshenko beam theory by Heckl et al. [34] and again in the wavenumber domain using a waveguide finite element model by Sheng et al. [35]. A combination of the wavenumber domain and the spatial domain is used by Zhang et al. [36].

Nilsson et al. [37] use the WFE method to reproduce the modal, high-frequency behaviour of a rail on a continuous support. In addition, the wavenumber boundary element method (WBEM) is applied to better capture the acoustic radiation from the

[4]The WFE method is sometimes called a 2.5D FE method, however, there is no reduction in dimensionality when transforming to the wavenumber domain. This approach will thus be referred to as the WFE method.

track along the length of the track. The presented method of combining the waveguide finite element method and the wavenumber boundary element method is frequently used to investigate the noise radiation of the rail (see e.g. [38, 39, 40]).

The presented papers **Paper A** and **Paper C** address the issue of a lacking, high-frequency model for slab track. In the WFE method, there is a considerable reduction of required degrees of freedom when reducing the mesh from 3D to 2D, which makes this method computationally advantageous when calculating large structures like the superstructure of a railway track. In this work, the WFE method has been implemented in an in-house code as described by Nilsson et al. [37]. This software has been applied to model both the vibrations in the rail as well as the rest of the superstructure. A method of introducing the discrete coupling between the two models has been implemented similar to the method presented by [36].

In this Section, the implemented WFE model of the rail is first compared to measurements of a ballasted track to validate the model and implementation for its use in rails. Then, a validation for the use of the WFE method to model the dynamic properties of the slab track is presented in a summary in **Paper C**.

3.2.1 WFE rail on simple support

For high-frequency vibrations, above about 1 kHz to 2 kHz depending on the rail and support stiffness, the rail is mostly decoupled from the vibrations in supporting structures like sleepers or slab. The receptance of the track then mainly depends on the receptance of the free rail. For frequencies below that, the receptance of the track is a product of the interaction between all the elements in the track superstructure. Nevertheless, a rather simple support model can accurately represent the track receptance in a large frequency range. This is shown in this section by creating a model of a UIC 60 rail using the implemented WFE method. This model is coupled to a simple support as described below, and compared to a measurement of a ballasted track, which was carried out by Thompson et al. [41] as part of the Roll2Rail project.

The WFE rail is coupled to an analytically calculated receptance in both vertical and lateral direction in three points across the foot of the rail. Along the track, the rail is coupled in 159 locations, using the concept described by Zhang et al. [36]. The analytical receptances are based on the assumption that the ballast and rail pad can be approximated by linear springs and the sleeper can be approximated by a simple mass. Damping is introduced by using a complex stiffness. Table 3.1 lists the parameters of the support and the rail. A principal sketch of the setup is shown in Figure 3.4. Note that only the elements relevant for the vertical direction are presented; an identical setup of springs exists for the lateral direction.

The receptance α is the chosen frequency response function to describe the response of the track. It is defined as the displacement η normalised with the harmonic force input F, $\alpha = \eta/F$. The derivation of the analytical expression for the receptance of the support is carried out in four steps following Figure 3.5.

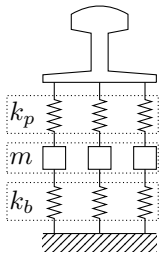

Figure 3.4: A principal sketch of the model setup.

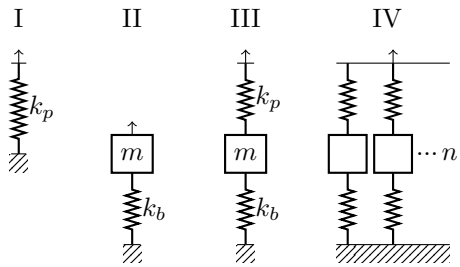

Figure 3.5: Steps in the derivation of the analytical expression for the foundation receptance at each contact node.

The receptance of the rail pad is modelled as a linear spring, thus the receptance is expressed as

$$\alpha_I = \frac{1}{k_p} \tag{3.1}$$

with the pad stiffness k_p. With the assumption of stationary harmonic excitation, the receptance at the top of the sleeper resting on the ballast is expressed as

$$\alpha_{II} = \frac{1}{k_b - m\omega^2} \tag{3.2}$$

with the ballast stiffness k_b and half the sleeper mass m. It is assumed that only half of the sleeper mass contributes to the dynamic system response. Coupling the receptances α_I and α_{II} in series is expressed as an addition,

$$\alpha_{III} = \frac{1}{k_p} + \frac{1}{k_b - m\omega^2} = \frac{k_p + \left(k_b - m\omega^2\right)}{k_p\left(k_b - m\omega^2\right)}. \tag{3.3}$$

This receptance could for example be used in combination with a single DOF beam model of the rail. However, the WFE produces results for flexural waves in three dimensions, so connecting a single degree of freedom along the width of the rail foot to α_{III} is likely inaccurate at higher frequencies. The continuous contact between the rail foot and the rail pad in lateral direction is instead approximated by coupling multiple (n) degrees-of-freedom (DOF) along the rail foot to the foundation.

Table 3.1: Parameters included in the simple support model.

	unit	vertical	lateral
Rail pad stiffness k_p	kN/mm	114	15.4
Rail pad damping coefficient η_p	-	0.25	0.08
Ground stiffness k_b	kN/mm	58	3.5
Sleeper mass m_s	kg	140	
Rail density ρ	kg/m^3	7850	
Rail poisson ratio ν	-	0.3	
Rail damping coefficient η	-	0.001	
Rail Young's modulus E	MPa	210	

However, coupling the rail to the receptance α_{III} multiple times does not produce the correct foundation stiffness. The partial receptance of each parallel strand α_{part} is introduced as a scaled version of α_{III} in order to achieve $\alpha_{IV} = \alpha_{III}$. With n identical (non-scaled) receptances α_{III} in parallel, their combined receptance α_{IV} is

$$\frac{1}{\alpha_{IV}} = n\frac{1}{\alpha_{III}} \rightarrow \alpha_{IV} = \frac{\alpha_{III}}{n}. \tag{3.4}$$

Thus, to approximate the receptance α_{III} with the setup in Figure 3.4, the partial receptance of each parallel strand needs to be multiplied with the number of strands n. The partial receptance α_{part} in one strand is thus described by

$$\alpha_{\text{part}} = n\alpha_{III} = \frac{n(k_p + k_b - \omega^2 m)}{k_p(k_b - \omega^2 m)} \tag{3.5}$$

where in this case, $n = 3$. The complex stiffness of the rail pad is evaluated as $k_p(1 + j\eta_p)$ and likewise for the ballast stiffness.

Figure 3.6 shows the implemented WFE model of the UIC 60 rail on ballasted track compared to the measurement [41] in terms of the vertical receptance. A close match is found between the measurement and the model. Especially the high-frequency behaviour of the rail is captured well. The same comparison is made for the lateral direction. In Figure 3.7, a very good correlation is found between the lateral rail receptances in the frequency range up to about 7 kHz. It is especially notable that the modal behaviour of the rail is captured well throughout this range.

One way to evaluate the decay of the vibration along the rail is the track decay rate. This quantity can especially be used as an indicator to estimate the noise emissions from the track [42]. Figures 3.8 and 3.9 show a comparison of the modelled and measured track decay rate and a close match is found here as well. In conclusion, it is found that the WFE model in combination with a simple analytical receptance for the support can provide a very good estimate of the behaviour of a ballasted track in the frequency range above about 80 Hz.

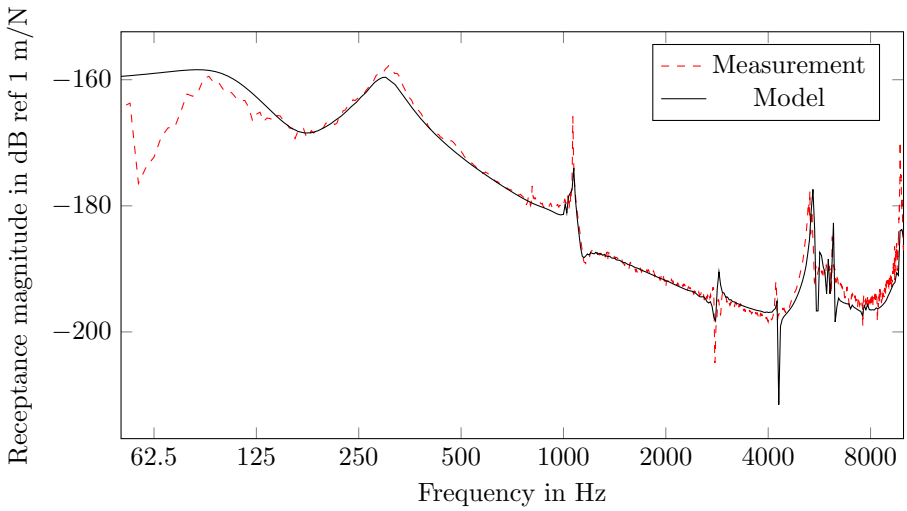

Figure 3.6: Vertical receptance of a UIC 60 rail on a ballasted track. The curve shows the vertical displacement response of the rail head when excited and measured at mid-span. A close match is achieved using the WFE model on a simple support.

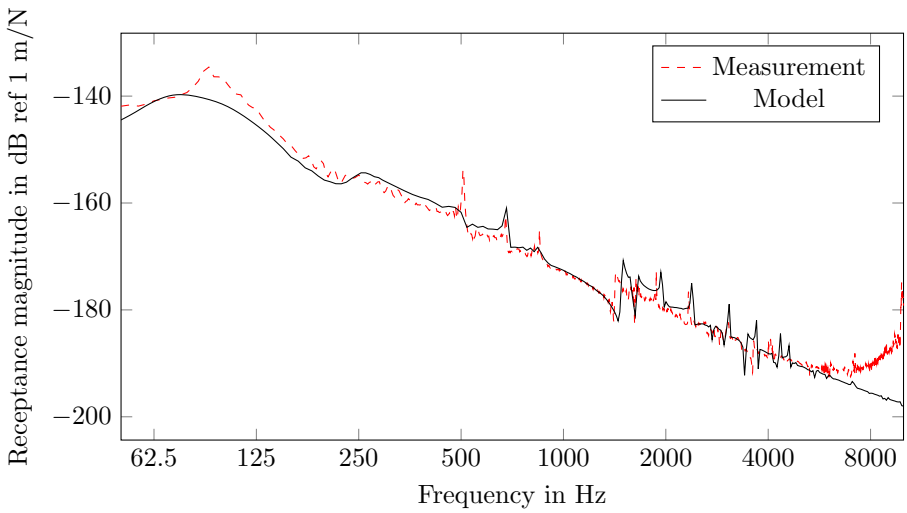

Figure 3.7: Lateral receptance of a UIC 60 rail on a ballasted track. The curve shows the lateral displacement response of the rail head when excited and measured at mid-span. A close match is achieved using the WFE model on a simple support.

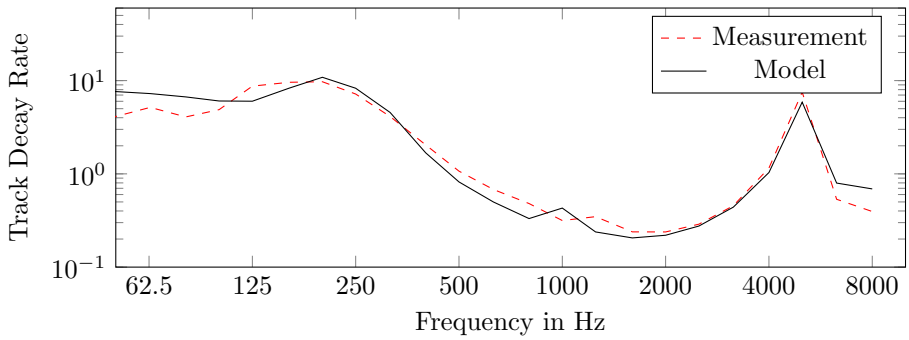

Figure 3.8: Vertical track decay rate of model and measurement.

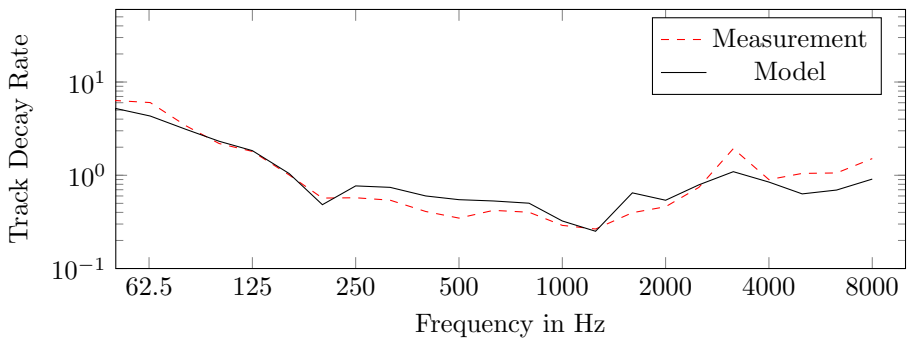

Figure 3.9: Lateral track decay rate of model and measurement.

3.2.2 WFE rail on WFE slab

Different models have been proposed for modelling the structural vibrations in slabs, e.g. based on beam theory [43], based on FEM using shell elements [44] or 3D brick elements [45], or a combination of FE and boundary elements (BE) [46]. A model based on the WFEM has been presented in [40]. The models based on 3D FEM and WFEM can likely fulfil the requirement on a high upper frequency limit for simulating noise radiation. An additional benefit of the WFEM is the lower computational cost and the inherent infinite extent of the track. In the following, a new method is presented based on discretely coupling two WFE models, which has been described in the appended **Paper A** and validated in **Paper C**. A similar approach followed in [40] uses the WFE model only for the slab and the layers below, but couples the slab to a beam model for the rail. The new modelling approach is summarised here.

In this method, the response of the free rail is evaluated using the WFE method. The response of the slab and the rest of the support layers is likewise evaluated using the WFE method. A section of the ground is included as a solid material, whose underside is fixed in space using Dirichlet boundary conditions. A principal sketch of the setup is shown in Figure 3.10. Notice the connection of the rail to the slab in three nodes across the rail foot. It is not necessary to use an equal spacing d_s of the rail seats in longitudinal direction [36].

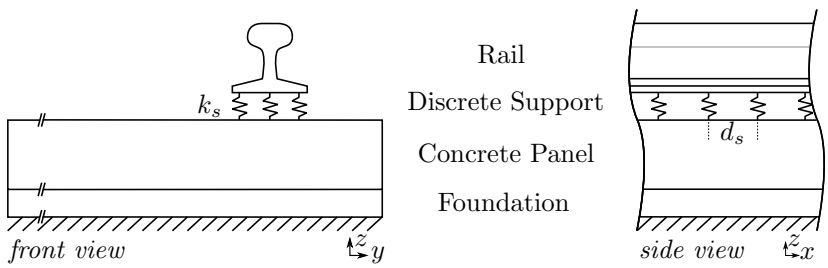

Figure 3.10: Sketch describing the discrete coupling of a rail with a concrete panel resting on a foundation. The combined spring stiffness k_s represents the rail pad stiffness. The spacing between the supports d_s can be varied.

The developed method as been implemented in the in-house WFEM code. To validate the modelling approach, the Chinese CRTS III track has been modelled. **Paper C** describes the realisation of this model in more depth. Further, validation measurements were conducted on a full-scale slab track test rig in the State Key Laboratory of Traction Power, South West Jiaotong University, Chengdu, China. Figure 3.11 shows the setup of the nodes of the 2D FE mesh, applied to the Chinese CRTS III slab track system shown in Figure 3.3. After conducting a parameter study and applying a genetic algorithm to calibrate the model parameters, a good match for multiple transfer functions is achieved. One such match is presented in Figure 3.12.

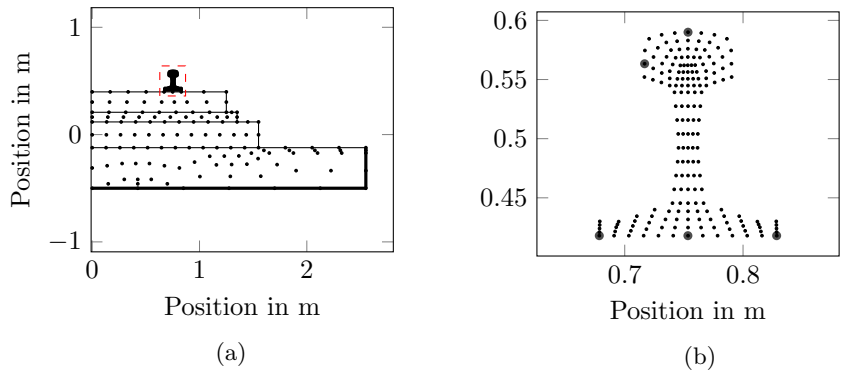

Figure 3.11: Nodes of the 2D finite element meshes of the CRTS III track system. (a) Track and rail. Note that only half of the symmetric mesh is shown. Top to bottom: Rail, slab, SCC layer, support layer, soil. Thick lines indicate a fixed boundary condition for the nodes on that boundary. The rail mesh is enlarged in (b). The nodes at which loads are applied are marked on the rail head. Likewise, nodes connected to the slab via springs are marked on the rail foot.

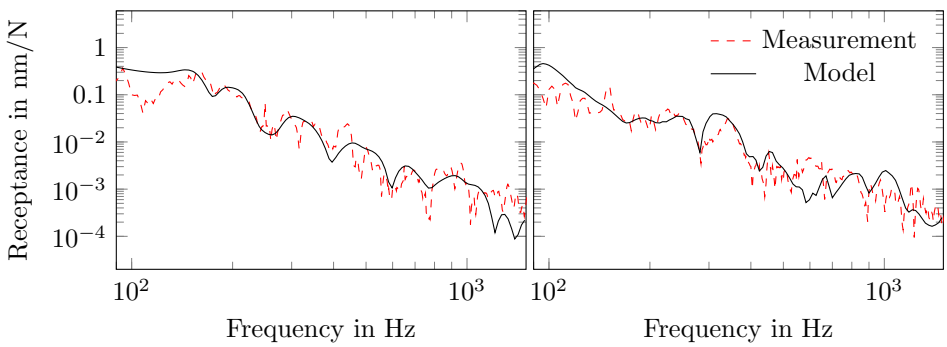

Figure 3.12: Comparison of the receptance magnitude for different excitation and measurement directions on the CRTS III track. The left and right figures show a vertical and a lateral receptance, respectively. The vertical receptance refers to a vertical excitation at the top node in Figure 3.11b, and the lateral receptance refers to an outward excitation at the node on the left side of the rail head. The response point is located on the slab, next to a rail seat.

3.3 Noise from slab tracks

Different methods for the sound radiation from rails and tracks are summarised in [15, Ch. 6.4]. One method combines the WFEM method presented above with the wavenumber boundary element method (WBEM). This was used by Nilsson et al. [37] for a free and an embedded rail and has since then been used in several other studies [24, 38, 39, 47]. In this work, the WBEM is used to calculate sound radiation from both the rail and the track.

In **Paper A**, the WFEM/WBEM approach is followed to calculate the sound radiation from the rail. However, instead of using only one BEM model, additionally, the vibrations from the concrete slab surface are included in the calculation. This enables the evaluation of the combined sound radiation from a slab track surface and the discretely supported rail. As described in Sec. 3.2.2, both the slab and the rail are modelled as WFE models. Therefore, the surface velocities of both bodies can be evaluated in wavenumber-frequency domain. The projection of these velocities on the surface normal direction produces the surface normal velocity which is then used as the input to the WBEM calculation.

In the paper, the transfer function for a unit force input at the top of rail to the total radiated sound power is evaluated. To identify parameters that influence the sound radiation from slab tracks, a parameter study is conducted focussing on (i) the rail pad stiffness, (ii) the thickness of the slab, and (iii) the type of support: continuous or discrete. It was found that similar to ballasted tracks, the rail pad stiffness has a major influence on the radiated sound power. By increasing this stiffness, a stronger coupling between the rail and its support is achieved. As pointed out by Thompson [15], this stronger coupling to the support decreases the vibration amplitude of the rail, increases the track decay rate, and ultimately leads to a lowered total radiated sound power. However, the rail pad stiffness is of major significance only for the discretely coupled rail. For a continuously supported rail, the total sound power is reduced and the rail pad stiffness is less influential.

In the WBEM, the slab and rail contributions are calculated separately. An evaluation of the contribution of the slab vibration to the total noise shows a minor significance of the noise produced by the slab surface. Nevertheless the slab can be expected to have a major influence on the directivity and the absorption characteristics of the radiated noise from the rails.

4 Railway wheel dynamics and noise modelling

This section addresses the modules related to the wheel in Figure 1.2. In Section 4.1, a description of commonly used models for the dynamics of railway wheels is given. Section 4.2 focusses on sound radiation from railway wheels.

4.1 Railway wheel dynamics

Analytical as well as numerical models have been applied to model the dynamic wheel response. In [48], the modes of vibration of a railway wheel are categorised like those of a flat circular plate. Consequently, the modes are described by their number of nodal diameters n and nodal circles m. This can be applied both to out-of-plane modes, also called axial modes, and in-plane modes, which could be either radial or circumferential modes. In this work the common notation to describe modes (n, m, a/r/c) is adopted with a, r and c for axial, radial and circumferential modes, respectively.

For numerical models, it is common to utilise the axi-symmetry of the structure. Thus, the size of the numerical problem can be drastically reduced by simplifying the geometry to its planar representation. Thompson [48] introduces a modelling approach based on the finite element method using axi-symmetric shell elements. In **Paper B**, an alternative modelling approach is applied to the case of a railway wheel, building on literature using the WFE method for curved structures for car tyres [49, 50]. Conceptually, here the wheel is considered an infinite waveguide with propagating waves around its axis of rotation. In contrast to straight waveguides, in which modes occur on a continuous wavenumber spectrum, here modes only occur at integer wavenumbers, due to the necessary continuity around the wheel.

Figure 4.1 presents the mesh of the cross-section of a railway wheel of type BA093 as e.g. used in the noise measurement car (Schallmesswagen, SMW) of DB Systemtechnik, described by Pieringer in [51]. The axle, indicated by the grey rectangle, is modelled as a rigid body. This approach was previously used by Thompson et al. [52], as it is pointed out in [48] that mainly the wheel modes of order $n = 0$ and $n = 1$ couple to the bending, extension and torsional modes of the axle. As, according to [52], these are not the main contributors to rolling noise, the dynamic properties of the axle can be ignored here.

The dynamic response of the wheel was evaluated using the WFE method for curved structures. The dispersion relation is shown in Figure 4.2. The dynamic response of the wheel at the contact point with the rail is described by its point mobilities, which are evaluated via modal superposition. The point mobility is the velocity response of the structure at a certain position, normalised by the corresponding harmonic excitation in the same position. Four modes are visualised in Figure 4.3.

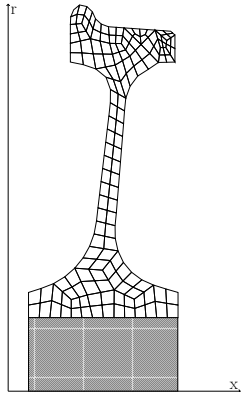

Figure 4.1: Finite element mesh of a railway wheel of the type BA093.

4.2 Noise from railway wheels

One convenient way to calculate the outward sound radiation in an unbounded domain is the Boundary Element Method (BEM). It is possible to formulate the method in cylindrical coordinates, see e.g. [53, 54]. There, the sound radiation is calculated using a Fourier series (FBEM), in which each element represents one order of the series. This method is used in Thompson et al. [52], where an engineering model for the sound radiated by railway wheels was developed. There, a key observation was that the radiation efficiency from lower order modes follows a power rule. In **Paper B**, this effect was reproduced using the in-house implementation of the FBEM. The connection to the power rule is visible for the radiation from the SMW wheel shown in Figure 4.1.

Figure 4.4 shows the radiation ratio for different numbers of nodal diameters and an axial excitation at the contact point. It is visible that the radiation ratio of each order n first follows a slope that is proportional to a f^{2n+2} and then tends towards unity for high frequencies. This is in line with [52] and further described in [15, Ch. 6.3].

The engineering models in [52] were developed for a wheel in free space. However, with the slab track surface in close proximity to the wheel, this assumption needs to be re-evaluated. In **Paper B**, a half-space formulation of the Green's functions is used in the BEM to account for ground reflection from an acoustically hard ground, i.e. a reflection factor $R = 1$. The acoustically hard ground could, for example, be a slab track surface or the street surface in an embedded rail tram system.

The radiation ratio of the wheel above an acoustically hard ground was evaluated using the developed model. Figure 4.5 shows the resulting radiation ratio. It was found that the presence of the track surface has the largest effect at low frequencies, up to about 200 Hz, leading to an increase of about 3 dB. Yet, the radiation ratio of the wheel is comparatively low in that frequency range. While it can be concluded that the slab track surface does not have a large impact on the radiation ratio, there can be a considerable influence on the directivity.

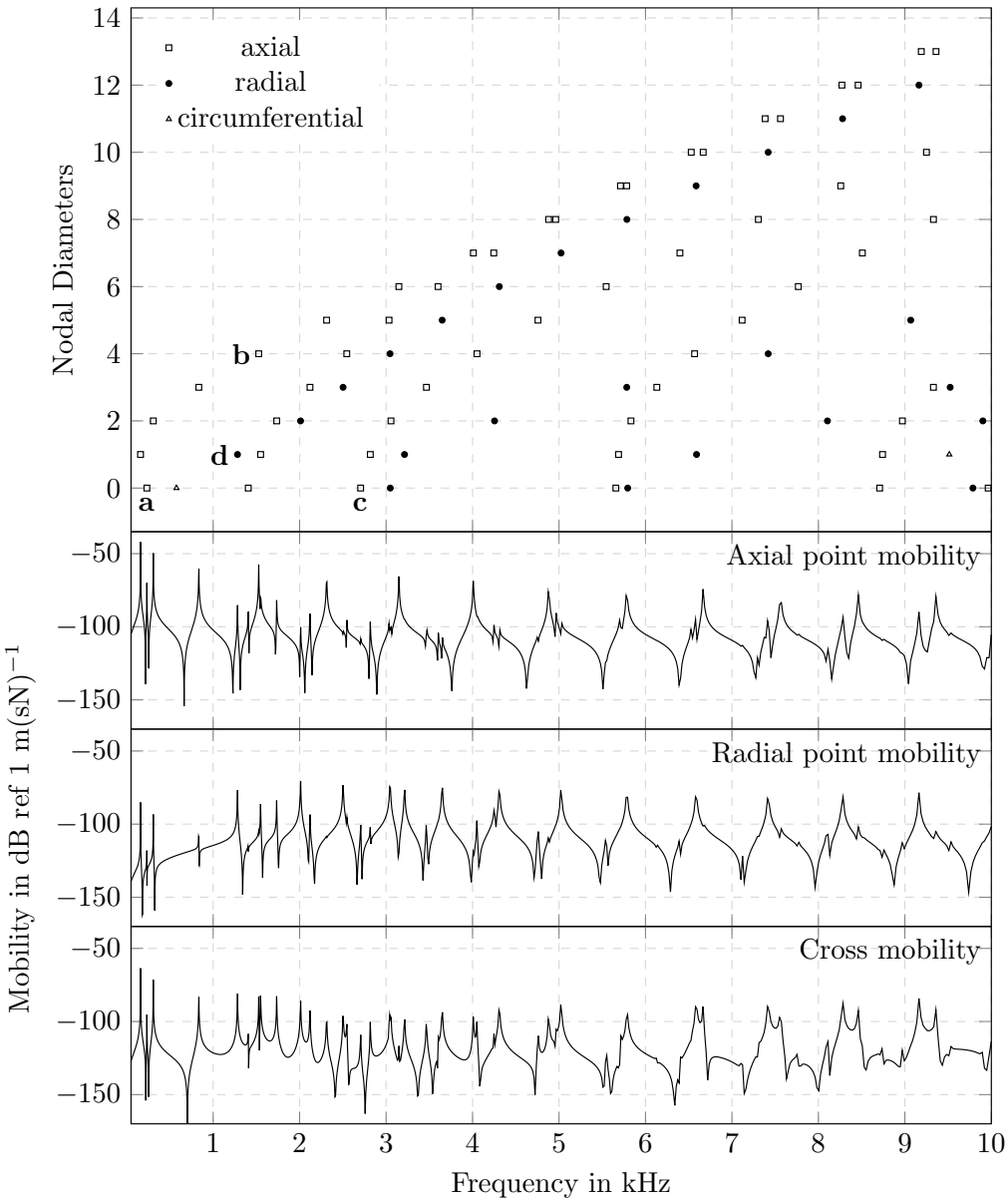

Figure 4.2: Top: Dispersion relation for the SMW wheel. Marked modes are **a**(0,0,a), **b**(4,0,a), **c**(0,2,a) and **d**(1,0,r). The lower figures show the axial, radial and axial/radial mobility at the contact point, centred on the running surface of the wheel.

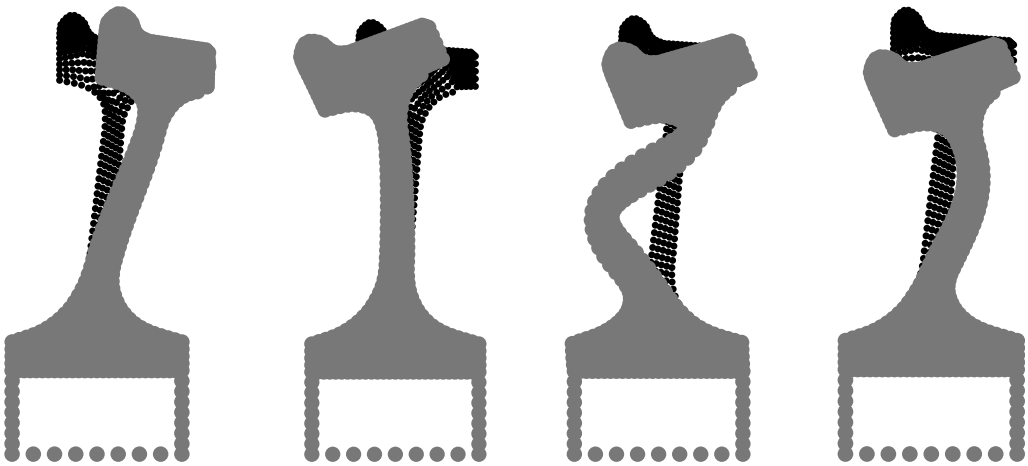

(a) (0,0,a) (b) (4,0,a) (c) (0,2,a) (d) (1,0,r))

Figure 4.3: Cross-sectional modal deflection shapes for the modes (a)-(d) indicated in Figure 4.2.

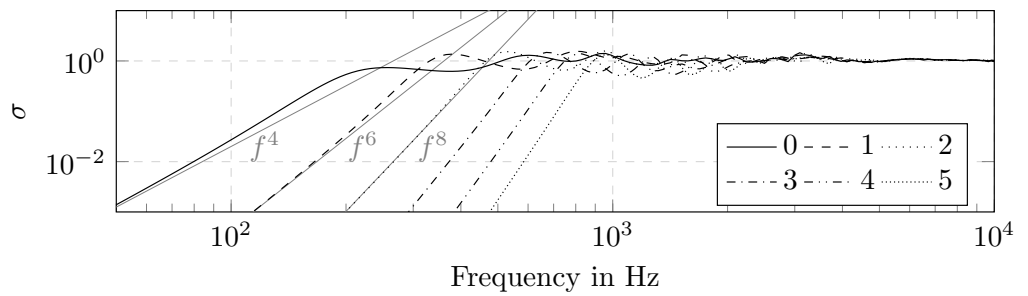

Figure 4.4: Radiation ratio σ of the wheel for different numbers of nodal diameters and an axial excitation at the contact point. The slopes of functions proportional to f^4, f^6 and f^8 are included as a reference.

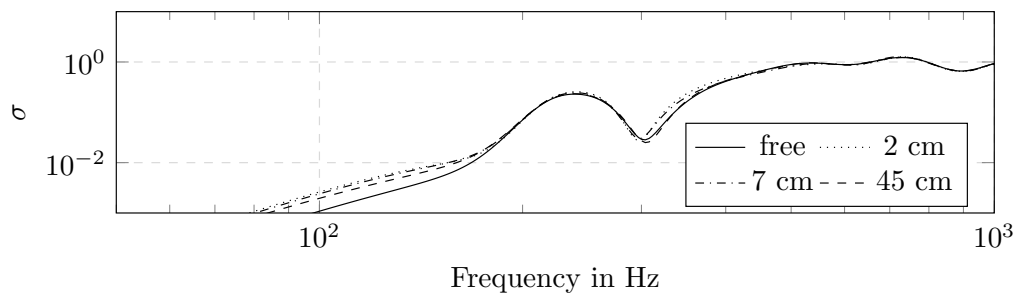

Figure 4.5: Radiation ratio for different heights of the wheel above the reflective surface.

5 Summary of appended papers

Paper A: The Influence of Track Parameters on the Sound Radiation from Slab Tracks

A frequency-wavenumber domain model for the dynamic response of slab tracks is developed including the discrete coupling of rail and slab. The surface velocities are used as the input to a wavenumber domain boundary element model. This enables the evaluation of the transfer function for a unit force input at the top of rail to the total radiated sound power. A parameter study is conducted focussing on (i) the rail pad stiffness, (ii) the thickness of the slab and (iii) the type of support: continuous or discrete. Comparable to ballasted tracks, an increasing rail pad stiffness is found to decrease the total radiated sound power. The rail pad stiffness is of major significance especially for the discretely coupled rail. For a continuously supported rail, the total sound power is reduced and the rail pad stiffness is less influential. The slab and rail contributions are calculated separately. An evaluation of the contribution of the slab vibration to the total noise shows a minor significance of the noise produced by the slab surface.

Paper B: Sound Radiation from Railway Wheels including Ground Reflections: A half-space formulation for the Fourier Boundary Element Method

This paper develops a method to evaluate the sound radiation from axi-symmetric bodies based on the curved Waveguide Finite Element and Fourier series Boundary Element Method. A half-space formulation of the Green's functions is applied in the Boundary Element Method to account for ground reflection from an acoustically hard ground. The acoustically hard ground could for example be a slab track surface or the street surface in an embedded rail tram system. The developed method is compared to analytical models as well as noise measurements of a vibrating steel disk. Using this method, the influence of the reflective plane on the radiation efficiency of railway wheels is researched. It is found that for the researched railway wheel, there is no major influence of the track surface on the radiation efficiency.

Paper C: Calibration and validation of two models for the dynamic response of slab track using data from a full-scale test rig

The calibration and validation of track dynamics simulation models is the focus in this paper. Impact hammer measurements were conducted on a full-scale slab track test rig in the State Key Laboratory of Traction Power, South West Jiaotong University, Chengdu, P.R. China. Then, both a finite and a waveguide finite element model are developed to represent a section of this track. The finite element model is three-dimensional where the rails are modelled as Rayleigh–Timoshenko beams and the concrete slab and support layer are modelled using linear plate elements. In the waveguide finite element model, a constant cross-section is assumed for the rail and the track, with the assumption of exponentially decaying, propagating waves along the track. The measurements are used to calculate the transfer functions between excitations on the rail and displacements on the slab and substructure. These receptances are then compared to the modelled version. A two step procedure is applied to calibrate the models, including (i) a parametric study

and (ii) a genetic algorithm. Finally, transfer functions from both calibrated models are compared to the measurements. A satisfactory agreement is found between the measured and calculated transfer functions, both for those TFs included in the calibration as well as others which were not included in the parameter matching. This implies that both models can successfully represent the dynamic properties of the test rig and can be considered as validated.

6 Conclusions

In this work, a numerical method for predicting vibrations in slab tracks has been developed, implemented and tested. The modelling approach is based on calculating frequency response functions separately in the rail and the rest of the superstructure in wavenumber-frequency domain, and then coupling the two systems in the positions of several rail seats in spatial-frequency domain. The developed method and implementation has been tested by comparison to measurements conducted on a full-scale slab track test rig, in which a good agreement was found.

Furthermore, the wavenumber boundary element method has been implemented to calculate the sound radiation from the vibrating structure. A simple slab track model has then been used to study the effect of track parameters such as the rail pad stiffness and the type of rail support (discrete/continuous). It was found that comparable to ballasted tracks, there is a large dependency of the radiated sound power to the rail pad stiffness, where an increased rail pad stiffness leads to a decreased radiated sound power. The contributions of the slab vibration to the total sound power was found low although relevant at low frequencies and for high rail pad stiffnesses.

Finally, a method for predicting the sound radiation from railway wheels over an acoustically hard reflective surface was developed, implemented and tested based on the axisymmetric Waveguide Finite Element method, and the Fourier series Wavenumber Boundary Element method combined with a half-space Green's functions approach. The implementation was tested against laboratory measurements and analytical models. A typical railway wheel geometry was modelled using this implementation. No significant change in the radiation efficiency of the wheel was found due to the presence of the surface. Note that this does not describe the influence of the reflecting surface on the directivity of the radiation but solely points at the fact that the total radiated sound power is not significantly affected by the slab surface.

7 Future Work

The components relevant to slab track will be integrated into one simulation tool according to the scheme presented in Figure 1.2. Specifically, a time-domain evaluation of the contact problem as presented by Pieringer [10, 55] will be used to generate realistic time-histories of wheel-rail interaction forces. A combination of the WFE and WBE method has been implemented in this work, tested and used to evaluate the transfer function from force input on the track to sound pressure level on the track-side. Combining this with the information of the time-history of the interaction forces will allow the modelling of track side noise levels during wheel pass-bys.

Further, a model for the vibration and radiation from ballasted track will be developed based on a similar approach as the model for slab track presented here. Then, a comparison of the radiation from ballasted and slab tracks will be conducted. The influence of the input parameters to the model will be researched. A validation of the model can be achieved by lab experiments and/or pass-by measurements on a real track.

Finally, the model will be applied to investigate two abatement measures for high noise levels. The first one, absorption on the track, provides a low profile solution that can potentially be retrofitted on existing tracks. A way to realise this is the introduction of an impedance plane in the developed Boundary Element model as described by Ochmann and Brick [56]. The second step is to investigate low-height barriers close to the track with regard to their acoustic performance, which can e.g. be achieved by introducing their geometry in the Boundary Element formulation.

References

[1] European Commission. Statistical Pocketbook 2019: EU transport. 2019.

[2] The European Commission. White Paper: Roadmap to a Single European Transport Area - Towards a competitive and resource efficient transport system. Retrieved May 17, 2020, from `https://eur-lex.europa.eu/legal-content/EN/TXT/PDF/?uri=CELEX:52011DC0144`. 2011.

[3] International Union of Railways (UIC). High speed Rail. Brochure. Retrieved May 8, 2020, from https://uic.org/passenger/highspeed. 2018.

[4] International Union of Railways (UIC). High Speed Traffic in the World. Document. Retrieved May 8, 2020, from https://uic.org/passenger/highspeed. 2020.

[5] C. Esveld. Modern Railway Track. Ed. by D. Zwarthoed-van Nieuwenhuizen. 2nd ed. Zaltbommel, The Netherlands: MRT-Productions. 2001.

[6] P. E. Gautier. Slab track: Review of existing systems and optimization potentials including very high speed. *Construction and Building Materials*. **92** (Feb. 2015), 9–15.

[7] ISO. *Acoustics — Description, measurement and assessment of environmental noise — Part 1: Basic quantities and assessment procedures*. Standard ISO 1996-1:2016(E). Geneva, Switzerland: International Organization for Standardization, 2016.

[8] International Union of Railways (UIC). UIC NETWORK NOISE & VIBRATION. Brochure. Retrieved May 8, 2020 from https://uic.org/IMG/pdf/uic_noise_flyer_2019.pdf. 2019.

[9] D. THOMPSON and C. JONES. A review of the modelling of wheel/rail noise generation. *Journal of Sound and Vibration*. **231**(3) (2000), 519–536.

[10] A. Pieringer, W. Kropp and D. J. Thompson. Investigation of the dynamic contact filter effect in vertical wheel/rail interaction using a 2D and a 3D non-Hertzian contact model. *Wear*. **271**(1-2) (2011), 328–338.

[11] D. Thompson. On the relationship between wheel and rail surface roughness and rolling noise. *Journal of Sound and Vibration*. **193**(1) (1996), 149–160.

[12] P. J. Remington. Wheel/rail noise-Part IV: Rolling noise. *Journal of Sound and Vibration*. (1976), 419–436.

[13] D. J. Thompson. Wheel-rail Noise Generation, Part I: Introduction And Interaction Model. *Journal of Sound and Vibration*. **161**(3) (Mar. 1993), 387–400.

[14] J. Nielsen and A. Igeland. Vertical dynamic interaction between train and track influence of wheel and track imperfections. *Journal of Sound and Vibration*. **187**(5) (1995), 825–839.

[15] D. Thompson. Railway Noise and Vibration. 1st ed. Oxford, United Kingdom: Elsevier Science. 2008.

[16] T. Kitawaga, K. Nagakura and T. Kurita. Contribution of Rolling Noise and Aerodynamic Noise to the Total Noise Generated from the Lower Part of Shinkansen Cars Running at High-speed. *Quarterly Report of RTRI.* **54**(4) (2013), 214–221.

[17] P. J. Remington. Wheel/rail rolling noise: What do we know? What don't we know? Where do we go from here? *Journal of Sound and Vibration.* **120**(2) (1988), 203–226.

[18] M. L. Munjal and M. Heckl. Vibrations of a periodic rail-sleeper system excited by an oscillating stationary transverse force. *Journal of Sound and Vibration.* **81**(4) (1982), 491–500.

[19] M. L. Munjal and M. Heckl. Some mechanisms of excitation of a railway wheel. *Journal of Sound and Vibration.* **81**(4) (1982), 477–489.

[20] R. J. Diehl, R. Nowack and G. Hölzl. Solutions for acoustical problems with ballastless track. *Journal of Sound and Vibration.* **231**(3) (2000), 899–906.

[21] S. Van Lier. Vibro-acoustic modelling of slab track with embedded rails. *Journal of Sound and Vibration.* **231**(3) (2000), 805–817.

[22] U. Moehler et al. The new German prediction model for railway noise "Schall 03 2006" -Potentials of the new calculation method for noise mitigation of planned rail traffic. *Notes on Numerical Fluid Mechanics and Multidisciplinary Design.* Vol. 99. (2008), 186–192.

[23] F. Poisson. "Railway Noise Generated by High-Speed Trains". *Notes on Numerical Fluid Mechanics and Multidisciplinary Design.* Vol. 126. Springer Verlag. 2015, pp. 457–480.

[24] X. Zhang et al. An engineering model for the prediction of the sound radiation from a railway track. *Journal of Sound and Vibration.* (Aug. 2019), 114921.

[25] E. Aggestam. Simulation of vertical dynamic interaction between railway vehicle and slab track. Licentiate Thesis. Gothenburg, Sweden: Chalmers University of Technology, 2018.

[26] Rail.One. RHEDA 2000® Ballastless Track System. Brochure. Retrieved on May 8, 2020, from https://www.railone.com/fileadmin/daten/05-presse-medien/downloads/broschueren/en/Rheda2000_EN_2011_ebook.pdf. Neumarkt, Germany, 2011.

[27] Rail.One. Getrac® Ballastless Track System. Brochure. Retrieved on May 8, 2020, from https://www.railone.com/fileadmin/daten/05-presse-medien/downloads/broschueren/en/Getrac_EN2012_ebook.pdf. Neumarkt, Germany, 2012.

[28] M. Wang et al. Experimental study on dynamic performance of typical nonballasted track systems using a full-scale test rig. *Proceedings of the Institution of Mechanical Engineers, Part F: Journal of Rail and Rapid Transit.* **231**(4) (2017), 470–481.

[29] Edilon)(sedra. One system crossing the boundaries. Brochure. Retrieved on May 8, 2020, from https://www.edilonsedra.com/ts-download/edilonsedra-corkelast-ers-embedded-rail-system-for-optimum-integration-into-tunnel-station-and-bridge-structures. Haarlem, The Netherlands, 2015.

[30] I. Avramovic, ÖBB-Porr. (Private communication). May 2020.

[31] D. J. Thompson, B. Hemsworth and N. Vincent. Experimental validation of the twins prediction program for rolling noise, part 1: Description of the model and method. *Journal of Sound and Vibration.* **193**(1) (1996), 123–135.

[32] D. J. Thompson. Wheel-rail Noise Generation, Part III: Rail Vibration. *Journal of Sound and Vibration.* **161**(3) (Mar. 1993), 421–446.

[33] L. Gavrić. Computation of propagative waves in free rail using a finite element technique. *Journal of Sound and Vibration.* **185**(3) (1995), 531–543.

[34] M. A. Heckl. Coupled waves on a periodically supported Timoshenko beam. *Journal of Sound and Vibration.* (2002), 849–882.

[35] X. Sheng, C. Jones and D. J. Thompson. Responses of infinite periodic structures to moving or stationary harmonic loads. *Journal of Sound and Vibration.* **282**(1-2) (2005), 125–149.

[36] X. Zhang et al. A model of a discretely supported railway track based on a 2.5D finite element approach. *Journal of Sound and Vibration.* **438** (2018), 153–174.

[37] C. M. Nilsson et al. A waveguide finite element and boundary element approach to calculating the sound radiated by railway and tram rails. *Journal of Sound and Vibration.* **321**(3-5) (2009), 813–836.

[38] X. Zhang, G. Squicciarini and D. J. Thompson. Sound radiation of a railway rail in close proximity to the ground. *Journal of Sound and Vibration.* **362** (2016), 111–124.

[39] X. Sheng, T. Zhong and Y. Li. Vibration and sound radiation of slab high-speed railway tracks subject to a moving harmonic load. *Journal of Sound and Vibration.* **395** (2017), 160–186.

[40] X. Zhang et al. The noise radiated by ballasted and slab tracks. *Applied Acoustics.* **151** (2019), 193–205.

[41] D. Thompson et al. Assessment of measurement-based methods for separating wheel and track contributions to railway rolling noise. *Applied Acoustics.* **140**(May) (2018), 48–62.

[42] C. Jones, D. Thompson and R. Diehl. The use of decay rates to analyse the performance of railway track in rolling noise generation. *Journal of Sound and Vibration.* **293**(3-5) (June 2006), 485–495.

[43] X. Yang et al. Effect of track irregularity on the dynamic response of a slab track under a high-speed train based on the composite track element method. *Applied Acoustics*. **99** (2015), 72–84.

[44] E. Aggestam, J. C. Nielsen and R. Bolmsvik. Simulation of vertical dynamic vehicle–track interaction using a two-dimensional slab track model. *Vehicle System Dynamics*. **56**(11) (2018), 1633–1657.

[45] E. Aggestam, J. C. O. Nielsen and N. Sved. Simulation of Vertical Dynamic Vehicle–Track Interaction – Comparison of Two- and Three-Dimensional Models. *Advances in Dynamics of Vehicles on Roads and Tracks*. Ed. by M. Klomp et al. Cham: Springer International Publishing. (2020), 415–422.

[46] P. Galvín, A. Romero and J. Domínguez. Vibrations induced by HST passage on ballast and non-ballast tracks. *Soil Dynamics and Earthquake Engineering*. **30**(9) (2010), 862–873.

[47] X. Zhang et al. The effects of ballast on the sound radiation from railway track. *Journal of Sound and Vibration*. **399** (July 2017), 137–150.

[48] D. J. Thompson. Wheel-rail Noise Generation, part II: Wheel Vibration. *Journal of Sound and Vibration*. **161**(3) (Mar. 1993), 401–419.

[49] S. Finnveden and M. Fraggstedt. Waveguide finite elements for curved structures. *Journal of Sound and Vibration*. **312**(4-5) (2008), 644–671.

[50] C. Hoever. The simulation of car and truck tyre vibrations, rolling resistance and rolling noise. PhD Thesis. Chalmers University of Technology, 2014, pp. 1–118.

[51] A. Pieringer. Acoustic monitoring of rail faults in the German railway network. *13th International Workshop on Railway Noise*. Ghent; (2019).

[52] D. J. Thompson and C. Jones. Sound radiation from a vibrating railway wheel. *Journal of Sound and Vibration*. **253**(2) (2002), 401–419.

[53] A. F. Seybert et al. A special integral equation formulation for acoustic radiation and scattering for axisymmetric bodies and boundary conditions. *Journal of the Acoustical Society of America*. (1986), 1241–1247.

[54] A. H. W. M. Kuijpers, G. Verbeek and J. W. Verheij. An improved acoustic Fourier boundary element method formulation using fast Fourier transform integration. *The Journal of the Acoustical Society of America*. **102**(3) (1997), 1394–1401.

[55] A. Pieringer. Time-domain modelling of high-frequency wheel / rail interaction. Ph.D. Thesis. Chalmers University of Technology, 2011.

[56] M. Ochmann and H. Brick. "Acoustical Radiation and Scattering above an Impedance Plane". *Computational Acoustics of Noise Propagation in Fluids - Finite and Boundary Element Methods*. Berlin, Heidelberg: Springer Berlin Heidelberg. 2008, pp. 459–494.